Innerworkings of Protein Purification: Binding of Ni, Cu, Co, Zn-iminodiacetic acid to Histidine Tags

Cole Donald; Brian Barngrover, PhD
Stephen F. Austin State University, Nacogdoches, Texas 75962

Abstract

Binding energy is the minimum energy required to keep an assembly of particles together or to separate an assembly of particles. This project involved analysis of the binding energies from various combinations of nickel, copper, cobalt and zinc-iminodiacetic acid (IDA) and histidine (His) tags. From the calculated enthalpy of the reactions, the theoretical binding energy required to keep the molecules together or to separate them, was determined. Binding involving a single contact between Ni, Cu, Co, and Zn-IDA and a string of histidine residues was determined to follow a trend, with the Zn complex being most favored. The reaction energies were not uniform for the single binding structures-from the single histidine to hexa-histidine. The penta-histidine tag was determined as the most stable form, making three binding contacts with the Ni-IDA assembly. To elute a bound hexa-histidine tag, all the three contact sites with [M]-IDA require competitive replacement with imidazole.

Introduction

Immobilized metal affinity chromatography (IMAC) is the most widely used purification method that separates proteins according to their affinity to metal ions.[1] In IMAC (Figure 1), the adsorption of proteins is based on the coordination between an immobilized metal-ion and an electron donor group from the protein surface.[2] Certain amino acids, e.g. histidine and cysteine, form complexes with the chelated metals around neutral pH (6–8) and it is primarily the histidine residues in a protein that are responsible for its binding to a chelated metal.[3] As seen in figure 2, Histidine tagged proteins have a high selective affinity for metal ions that can be immobilized on chromatographic media using chelation ligands.[4] The most commonly used are transition metal-ions, Cu(II), Zn(II), Co(II), Fe(III), and especially Ni(II).

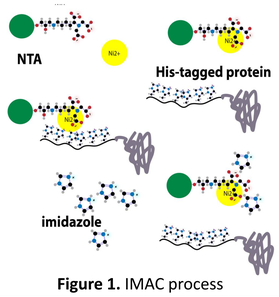

Figure 1. IMAC process

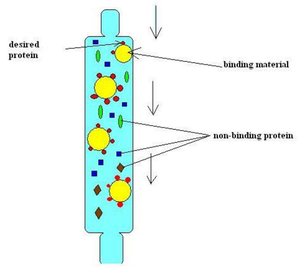

Figure 2. IMAC column

Computational Details

All calculations are performed with the Amsterdam Density Functional (ADF)[6] package, using density functional theory with the Becke Perdew (BP86)[7,8] functional and a frozen-core polarized triple-ζ (TZP) basis set. Scalar relativistic effects are included by employing the Zero Order Regular Approximation (ZORA).[9] The methanol solvent is incorporated using the Conductor-like Screening Model (COSMO), which represents the solvent by its dielectric constant.[10-13]

Table 1. Comparison of Ni^{2+}, Co^{2+}, Cu^{2+}, Zn^{2+}-IDA, and histidine reaction energies.

Structures	Ni^{2+} Reaction Energy (eV)	Co^{2+} Reaction Energy (eV)	Cu^{2+} Reaction Energy (eV)	Zn^{2+} Reaction Energy (eV)
$[M]^{2+}$ IDA histidine complex	-1.19	-0.87	-1.24	-1.89
$[M]^{2+}$ IDA dihistidine complex	-1.58	-1.50	-1.42	-2.16
$[M]^{2+}$ IDA trihistidine complex	-1.43	-1.47	-1.45	-2.13
$[M]^{2+}$ IDA tetrahistidine complex	-1.25	-1.23	-1.13	-1.80
$[M]^{2+}$ IDA pentahistidine complex	-1.61	-2.10	-2.02	-2.71
$[M]^{2+}$ IDA hexahistidine complex	-1.15	-1.10	NA	-2.13

Table 2. Comparison of Ni^{2+}, Co^{2+}, Cu^{2+}, Zn^{2+}-IDA, and imidazole reaction energies.

Structures	Ni^{2+} Reaction Energy (eV)	Co^{2+} Reaction Energy (eV)	Cu^{2+} Reaction Energy (eV)	Zn^{2+} Reaction Energy (eV)
$[M]^{2+}$ + One Imidazole	-0.92	-0.97	-0.99	-0.90
$[M]^{2+}$ + Two Imidazole	-1.99	-1.87	-1.79	-1.52
$[M]^{2+}$ + Three Imidazole	-2.87	-2.64	-2.26	-1.86

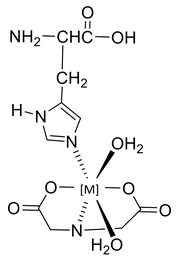

Figure 3. $[M]^{2+}$ IDA histidine complex

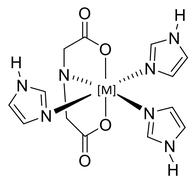

Figure 5. $[M]^{2+}$ IDA tri-Imidazole complex

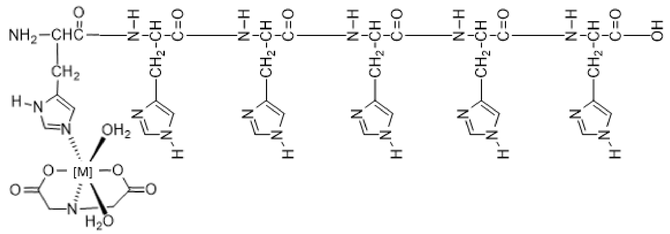

Figure 4. $[M]^{2+}$ IDA hexahistidine complex

Results

This study focuses on the incremental binding energy of histidine tags. The tag sizes range from a single histidine to six histidines. However, for completeness of the study a single histidine binding to [M]-IDA is examined (Figure 3). The calculated binding energy of a single histidine in the 1 or 3 position on the Ni^{2+} is -1.19 eV, -0.87 eV for Co^{2+}, -1.24 eV for Cu^{2+} and -1.89 eV for Zn^{2+}. As this shows that the reaction is favored, it is known that a single histidine is far too reactive to exist in nature, because histidines form oligopeptides. The calculated binding energy of the di-his chain at the 1 position on the Ni^{2+} is -1.58 eV, -1.50 eV for Co^{2+}, -1.42 eV for Cu^{2+} and -2.16 eV for Zn^{2+}. The calculated binding energy of the tri-his chain at the single binding site at the 1 position on the Ni^{2+} is -1.43 eV, -1.47 eV for Co^{2+}, -1.45 eV for Cu^{2+} and -2.13 eV for Zn^{2+}. The calculated binding energy of the tetra-his chain at the single binding site at the 1 position on the Ni^{2+} is -1.25 eV, -1.23 eV for Co^{2+}, -1.13 eV for Cu^{2+} and -1.80 eV for Zn^{2+}. The calculated binding energy of the penta-his chain at the single binding site at the 1 position on the Ni^{2+} is -1.61 eV, -2.10 eV for Co^{2+}, -2.02 eV for Cu^{2+} and -2.71 eV for Zn^{2+}. The calculated binding energy of the hexa-his chain at the single binding site at the 1 position on the Ni^{2+} is -1.15 eV , -1.10 eV for Co^{2+}, undetermined for Cu^{2+} and -2.13 eV for Zn^{2+} (Figure 4).

Discussion

The trends as seen in (Table 1) show that the reaction energy of the single binding complexes slightly increases from a single histidine to a di-histidine tag but remains nearly constant from the di-histidine to the hexa-histidine tag. The Zn-IDA complexes are more favorable compared to the other metal-IDA complexes. All the [M]-IDA complexes share a similar trend in reaction energies. The penta-histidine tag was determined as the most stable form, making three binding contacts with the Ni-IDA assembly. The trends as seen in (Table 2) show the reaction energies for imidazole binding to one, two, and all three of the sites on [M]-IDA (Figure 5).

Conclusions

From the data, it was determined that the Zn-IDA complex is more favorable than the other metal complexes. The reaction energies for the single binding structures were relatively not uniform from the single histidine to the hexa-histidine. Although, all complexes shared an overall trend. As shown by the research group from the La Roche corporation, the hexa-histidine tag was the most favored structure. In order to elute the histidine tag from the [M]-IDA, all three sites on the $[M]^{2+}$ ion must be replaced by imidazole

Contact

Cole Donald
Department of Chemistry and Biochemistry, Stephen F. Austin State University
Bush Mathematical Sciences Building, Nacogdoches, Texas 75962
donaldcb@jacks.sfasu.edu
903-754-9211

References

1. Saraswathy, N.; Ramalingam, P. Concepts and Techniques in Genomics and Proteomics, Woodhead Publishing Series in Biomedicine, 2011; pp 203-211.
2. Gutiérrez, R.; Del Valle, E. M.; Galán, M. A. Immobilized Metal-Ion Affinity Chromatography: Status and Trends. Separation & Purification Reviews, 2007, 36, 71-111. DOI:10.1080/15422110601166007
3. Immobilized Metal Chelate Affinity Chromatography (IMAC) (Sigma-Aldrich). https://www.sigmaaldrich.com/technical-documents/protocols/biology/affinity-chromatography/metal-chelate-afnity-chromatography.html (accessed June 2019).
4. GE Healthcare Life Sciences (2012) Recombinant Protein Purification, GE Healthcare Bio-Sciences AB, Uppsala, Sweden, pp 27.
5. NTA versus IDA: What's the Difference? (Cube Biotech). https://cube-biotech.com/us/nta-versus-ida-what-s-the-difference (accessed June 2019).
6. te Velde, G.; Bickelhaupt, F. M.; Baerends, E. J.; Fonseca Guerra, C.; van Gisbergen, S. J. A.; Snijders, J. G.; Ziegler, T. Chemistry with ADF. J. Comput. Chem. 2001, 22, 931-967.
7. Becke, A. D. Density-Functional Exchange-Energy Approximation with Correct Asymptotic Behavior. Phys. Rev. A. 1988, 38, 3098-3100.
8. Perdew, J. P. Density-Functional Approximation for the Correlation Energy of the Inhomogeneous Electron Gas. Phys. Rev. B. 1986, 33, 8822-8824.
9. van Lenthe, E.; Ehlers, A.; Baerends, E.-J. Geometry Optimizations in the Zero Order Regular Approximation for Relativistic Effects. J. Chem. Phys. 1999, 110, 8943-8953.
10. Klamt, A.; Schüürmann, G. COSMO: A New Approach to Dielectric Screening in Solvents with Explicit Expressions for the Screening Energy and its Gradient. J. Chem. Soc. Perkin Trans. 2. 1993, 799-805.
11. Pye, C. C.; Ziegler, T. An Implementation of the Conductor-Like Screening Model of Solvation within the Amsterdam Density Functional Package. Theor. Chem. Acc. 1999, 101, 396-408.
12. Klamt, A. Conductor-like Screening Model for Real Solvents: A New Approach to the Quantitative Calculation of Solvation Phenomena. J. Phys. Chem. 1995, 99, 2224-2235.
13. Klamt, A.; Jonas, V. Treatment of the Outlying Charge in Continuum Solvation Models. J. Chem. Phys. 1996, 105, 9972-9981.